Plant Physiol. (1997) 115: 803–815

Quantum Yields and Rate Constants of Photochemical and Nonphotochemical Excitation Quenching[1]

Experiment and Model

Agu Laisk*, Vello Oja, Bahtijor Rasulov, Hillar Eichelmann, and Astrid Sumberg

Tartu Ülikooli Molekulaar-ja Rakubioloogia Instituut, Riia tn. 181, Tartu, EE2400, Estonia (A.L., V.O., H.E., A.S.); and Institute of Plant Physiology and Genetics, Academy of Sciences, Dushanbe 734063, Tajik Republic (B.R.)

Sunflower (*Helianthus annuus* L.), cotton (*Gossypium hirsutum* L.), tobacco (*Nicotiana tabacum* L.), sorghum (*Sorghum bicolor* Moench.), amaranth (*Amaranthus cruentus* L.), and cytochrome b_6f *complex*-deficient transgenic tobacco leaves were used to test the response of plants exposed to different light intensities and CO_2 concentrations before and after photoinhibition at 4000 μmol photons m^{-2} s^{-1} and to thermoinhibition up to 45°C. Quantum yields of photochemical and nonphotochemical excitation quenching (Y_P and Y_N) and the corresponding relative rate constants for excitation capture from the antenna-primary radical pair equilibrium system (k'_P and k'_N) were calculated from measured fluorescence parameters. The above treatments resulted in decreases in Y_P and k'_P and in approximately complementary increases in Y_N and k'_N under normal and inhibitory conditions. The results were reproduced by a mathematical model of electron/proton transport and O_2 evolution/CO_2 assimilation in photosynthesis based on budget equations for the intermediates of photosynthesis. Quantitative differences between model predictions and experiments are explainable, assuming that electron transport is organized into domains that contain relatively complete electron and proton transport chains (e.g. thylakoids). With the complementation that occurs between the photochemical and nonphotochemical excitation quenching, the regulatory system can constantly maintain the shortest lifetime of excitation necessary to avoid the formation of chlorophyll triplet states and singlet oxygen.

In photosynthesis quanta are absorbed by chlorophylls surrounding PSII and PSI, where excitations (excitons) are created. The bulk of the chlorophyll forms a light-harvesting complex at PSII, which is connected with the reaction center via smaller peripheral antennae CP26, CP24, and CP29 (Dainese et al., 1992; Green and Durnford, 1996). Excitons diffuse in light-harvesting complex at PSII by hopping from chlorophyll to chlorophyll by a resonance mechanism or by a faster coherent mechanism, occasionally visiting the reaction center chlorophyll *P*680, where an exciton can mediate charge separation to form at first the primary radical pair $P680^+/Pheo^-$ (for review, see Krause and Weis, 1991; Renger, 1992; van Grondelle et al., 1994; Lavergne and Trissl, 1995). The primary radical pair is reversible and the exciton can be returned to the antenna. Alternatively, the separated charges can be stabilized by transferring the electron to Q_a. Exciton equilibration occurs about an order of magnitude faster (10–15 ps) than the actual lifetime of excitation (150–300 ps). Although the charge separation process itself occurs within about 3 ps, the reaction center chlorophyll shares the excitation with other chlorophylls, which reduces approximately proportionally the probability for charge separation, increasing the lifetime of excitation to about 150 to 300 ps. If Q_a is singly reduced, the redox potential of the $P680^+/Pheo^-$ radical pair decreases due to electrical repulsion, which shifts the equilibrium toward the antenna (van Mieghem et al., 1995), slowing the double reduction of Q_a.

According to this model, the rate-limiting step is charge separation plus stabilization on Q_a, which is slower the larger the antenna. In most cases the radical pair rapidly recombines and an exciton continues diffusing around until it is either quenched by thermal conversion or emitted as fluorescence. The quantum yield of fluorescence is propor-

[1] This work was supported by Estonian Science Foundation grant no. 1808, in Italy by Consiglio Nazionale delle Ricerche-North Atlantic Treaty Organization guest fellowship no. 217.27/1.06 while A.L. was a visiting fellow at IBEV (Consiglio Nazionale delle Ricerche), and in the United States by National Science Foundation grant no. IBN 9317756 while A.L. was a visiting fellow at Washington State University.

* Corresponding author; e-mail laisk@zbi.tartu.ee; fax 372–7–420286.

Abbreviations: Cyt b_6f, Cyt b_6f complex; ΔpH, pH gradient; F, steady-state fluorescence yield in the dark; F', steady-state fluorescence yield in the light; F'_m, pulse-saturated fluorescence yield in the light; F_{max}, highest pulse-saturated fluorescence yield in the dark-adapted state; F'_o, (lowest) fluorescence yield with open PSII centers; k_d, k_f, absolute rate constants for thermal dissipation of excitation and fluorescence, respectively; k_{Nm}, maximum possible k_N in numeric experiments; k'_P, k'_N, relative rate constants for excitation quenching by photochemistry and by regulated thermal dissipation, respectively; k'_{PO}, k'_P when all reaction centers are open; Pheo, the pheophytine acceptor of PSII; PPAD, photosynthetic photon absorption density; PQ, plastoquinone; *P*680, PSII center chlorophyll; Q_a, the quinone acceptor of PSII; q_P, photochemical excitation quenching; q_N, q_E, q_I, total nonphotochemical, energy-dependent, and inhibitory excitation quenching, respectively; Y_N, quantum yield (probability) of regulatory nonphotochemical excitation quenching; Y_P, quantum yield of photoreaction (of PSII electron transport).

tional to the average lifetime of an exciton. The yield of fluorescence is high (F'_m) when the PSII acceptor side is closed (Q_a is reduced and the lifetime of the exciton is long), and low (F'_o) when it is open (Q_a is oxidized and the lifetime of the exciton is short). The acceptor Q_a can be reduced by applying very high-intensity light that far exceeds the possible rate of Q_a oxidation. However, under sustained high-intensity light F' is not stable and soon decreases to about the same level as it was under low light. This shows that as photochemical quenching is disabled, another nonphotochemical quenching of excitation (q_N) is enabled to substitute for photochemical quenching. As a result, the lifetime of excitation remains almost constant when conditions for photosynthesis change, and the probability of uncontrolled production of oxidants and reductants that may lead to damaging reactions is constantly kept at a minimum (Horton et al., 1988; Foyer et al., 1990).

One component of the q_N, the q_E, is rapidly reversed at low light intensity, since it is related to the acidification of the thylakoid lumen (Krause and Weis, 1991; Horton et al., 1996). However, after a sufficiently long exposure under high light (photoinhibition) or high temperature (thermoinhibition), q_I is persistent for many hours (Havaux, 1993; for review, see Osmond, 1994). Proposed mechanisms for the energy-dependent and inhibitory quenching are different; the first is induced in the antenna via membrane energization in the presence of zeaxanthin, whereas the second is caused by damage (weakening) of the water-splitting apparatus (Prasil et al., 1992; Havaux, 1993; Horton et al., 1996). In this work we compare quantum yields (probabilities), Y_P and Y_N, and relative rate constants, k'_P and k'_N, of photochemical and nonphotochemical quenching in different uninhibited and in thermoinhibited and photoinhibited leaves. We show that the relationship between these parameters is similar and independent of the way the quenching is induced. Under most conditions normally the relationship between Y_P and Y_N and k'_P and k'_N is approximately complementary, showing an efficient control of the lifetime of excitation. However, under some conditions in which the proton gradient and zeaxanthin formation may be limited, nonphotochemical quenching is not able to completely substitute for the decreasing photochemical quenching. The experiment results will be compared with model simulations.

MATERIALS AND METHODS

Sunflower (*Helianthus annuus* L.) plants used in thermoinhibition experiments were grown in 2-L pots in growth cabinets (Sanyo-Gallempkamf, Loughborough, UK) at 18/15°C and 28/18°C day/night temperatures, at 1000 μmol quanta m^{-2} s^{-1} at the Institute of Plant Biochemistry and Ecology (IBEV-CNR) near Rome. Plants were watered daily to soil saturation and commercial liquid fertilizer was added to the water twice a week. Cotton (*Gossypium hirsutum* L.) and sunflower used in photoinhibition experiments were grown in Tartu (Estonia) in a homemade growth cabinet in 4-L pots in a peat-soil mixture with adequate nutrition at 25/20°C and 14-/10-h day/night regime and a PPFD of 650 μmol quanta m^{-2} s^{-1}. Wild-type and transgenic Cyt b_6f-deficient tobacco (*Nicotiana tabacum* L.) (Price et al., 1995) was grown in the same growth cabinet under 170 to 250 (referred to as low-light-grown) and 570 (high-light-grown) μmol quanta m^{-2} s^{-1}. Attached leaves of 30- to 40-d-old plants were used in experiments. C_4 plants *Sorghum bicolor* (Moench.) and *Amaranthus cruentus* (L.) were grown in a commercial soil containing peat moss, vermiculite, and sand (2:1:1) in 4-L pots in a greenhouse at Washington State University, Pullman, at 30/24°C day/night temperatures under normal sunlight plus sodium vapor lamps with maximum daily PPFD of about 1500 μmol quanta m^{-2} s^{-1} on sunny days.

Gas Conditioning

Single leaves were enclosed in a chamber (diameter, 31 mm; height, 3 mm) and exposed to a gas flow rate of 0.5 mmol s^{-1}. The upper side of the leaf was sealed with agar gel to the thermostated glass window to stabilize leaf temperature within ±0.5°C to that of the water bath. CO_2 exchange and transpiration were recorded in parallel with fluorescence measurements to quantify the photosynthetic activity. Different O_2 concentrations were obtained by mixing O_2 and N_2 at controlled rates. Water vapor pressure was controlled by passing a part of the flow over water warmed to 50°C; water vapor pressure difference between the leaf and gas was constant at 15 mb independent of temperature. Different CO_2 concentrations were obtained by mixing pure CO_2 into the gas flow through a capillary under controlled pressure difference.

Fluorescence Measurements

The leaf chamber was illuminated through a homemade light guide of plastic fibers 1 mm in diameter (Toray polymer optical fiber, PF-series, Laser Components, Gröbenzell, München, Germany). By individual arrangement of each fiber, light from two sources (Schott KL 1500, from Heinz Walz, Effeltrich, Germany) was evenly superimposed over the leaf area. One KL 1500 lamp provided 2-s pulses of 13,000 μmol quanta m^{-2} s^{-1} for fluorescence saturation and the other was used for actinic illumination. Far-red light was obtained from the same source through an interference filter with maximum at 720 nm. Voltage control and neutral density filters were used to reduce the light intensity, which was measured by a LI-189 quantum sensor (Li-Cor, Lincoln, NE). Using the same fiber arrangement, chlorophyll fluorescence was measured from a 10 × 20 mm^2 spot on the leaf with a pulse-amplitude-modulated fluorometer PAM 101 (Heinz Walz). A 1.6-kHz pulse frequency was used at low actinic light and in the dark.

Experimental Routines

In the beginning of the experiments leaves were dark adapted and F_{max} was measured by applying a saturation flash. Then stomata were allowed to open and photosynthesis was stabilized at a light intensity of 1300 μmol m^{-2} s^{-1} in 295 (experiments with sorghum and amaranth) or 330 μmol mol^{-1} CO_2 and 21% O_2. Thereafter, different CO_2

concentrations, O_2 concentrations, and light intensities were applied to the leaf. The exposure under each particular condition lasted 4 to 5 min until CO_2 fixation, photorespiration, and energy-dependent fluorescence quenching stabilized. Then a saturation flash was applied to obtain F'_m and about 10 s later the actinic light was replaced by far-red illumination for 5 s to obtain F'_o. Under the far-red light the recording trace rapidly dropped to a minimum in about 0.5 s and then started to increase (probably because of relaxation of the pH gradient). The minimum of the recording was taken for F'_o. Between exposures to different gas mixtures the leaf was allowed to regain the original net CO_2 fixation rate at 300 μmol mol^{-1} CO_2 and 21% O_2. Light-response curves were measured in sequence of decreasing PPADs, to avoid stomatal limitation. The dark-adapted F_{max} obtained after the measurement of the light curve was usually less than F_{max} measured before the exposure of the leaf to saturating light intensities; therefore, F_{max} measured in the beginning of the experiment was used as the uninhibited maximum fluorescence yield. However, in experiments with transgenic tobacco and C_4 plants, F_{max} was not measured in the beginning of the experiment and the F_m obtained after the measurement of the light-response curve was used as F_{max}. For this reason, in these experiments F_{max} was probably underestimated, but this only apparently decreased the sum of $Y_P + Y_N$ and $k'_P + k'_N$ (because a part of k_N was considered as k_d) and did not influence the complementation of the two quantum yields.

In thermoinhibition experiments the routine was repeated at different temperatures. At elevated temperatures the measurements were not commenced before stomatal opening and photosynthesis was stabilized. In photoinhibition experiments this routine was repeated before and after photoinhibition at 4000 μmol m^{-2} s^{-1} for different lengths of time. In some experiments F_m and F were measured in the dark after photoinhibition or thermoinhibition and used for the calculation of Y_P and Y_N in the dark-adapted state.

Calculation of Quantum Yields and Rate Constants for Excitation Quenching

For a system with well-connected PSII units in which competitive quenchers capture excitation from a large total pool, the main equation describing fluorescence in terms of the rate constants of excitation capture is:

$$F' = \frac{k'_f}{1 + k'_P + k'_N}. \quad (1)$$

In Equation 1 and below we introduce relative rate constants $k'_j = k_j/(k_f + k_d)$, where j = f, P, or N. The rate constants for fluorescence emission, k_f, and for basic nonradiative excitation decay in the pigment bed, k_d, are usually considered invariant in fluorescence analyses, so in this work we have made use of this constancy and have expressed other rate constants relative to the sum of the two. Physically, this means that the absolute rate constant for photochemical energy conversion from the total pigment bed to stabilized charges, k_P, and the absolute regulated rate constant for nonphotochemical excitation quenching, k_N, are expressed relative to the basic physical excitation decay rate. These relative rate constants, like the absolute rate constants, are related to measured fluorescence values, except that now $k_f + k_d = 1$. When k'_P is turned to 0 by a saturating flash of light, Equation 1 becomes:

$$F'_m = \frac{k'_f}{1 + k'_N} \quad (2)$$

Assuming that $k'_N = 0$ in a dark-adapted, uninhibited leaf, the maximum possible pulse-saturated fluorescence yield is F_{max}:

$$F_{max} = k'_f \quad (3)$$

Combining Equations 1 and 2, an expression for the quantum yield of photochemical excitation quenching in terms of F' and F'_m was obtained (Genty et al., 1989):

$$Y_P = 1 - \frac{F'}{F'_m} = \frac{k'_P}{1 + k'_P + k'_N} \quad (4)$$

Combining Equations 1, 2, and 3, the following expression for the quantum yield of nonphotochemical quenching that occurs concurrently and competitively with photochemical quenching has recently been derived (Genty et al., 1996):

$$Y_N = \frac{F'}{F'_m} - \frac{F'}{F_{max}} = \frac{k'_N}{1 + k'_P + k'_N} \quad (5)$$

We express the relative rate constants through measurable fluorescence terms as follows:

$$k'_N = \frac{F_{max}}{F'_m} - 1 \quad (6)$$

and

$$k'_P = \frac{F_{max}}{F'} - \frac{F_{max}}{F'_m} \quad (7)$$

Equation 7 accounts for the changes in k'_P caused by acceptor-side reduction in some PSII centers. To detect changes in k'_{PO} of open centers, F_o has to be used instead of F:

$$k'_{PO} = \frac{F_{max}}{F'_o} - \frac{F_{max}}{F'_m} \quad (8)$$

Modeling Nonphotochemical Quenching

The general model of photosynthesis (Laisk and Eichelmann, 1989; Laisk et al., 1989; Laisk and Walker, 1989; Laisk, 1993), in which transmembrane ΔpH is a parameter, was used for modeling nonphotochemical excitation quenching by introducing the following changes. PSII and PSI have donor (D) and acceptor (A) side carriers that can be reduced or oxidized. As a result, each of the photosystems is a sum of the following partial states: $A = D^-A^-$; $B = D^-A^+$; $C = D^+A^-$; $D = D^+A^+$. Conversions between

the states are characterized by the corresponding rate constants: for donor-side re-reduction after oxidation (j), for acceptor-side oxidation after reduction (q), and for electron transfer from the donor to the acceptor side (n). All of these reactions are allowed to reverse (constants are denoted by primes). The rate constant for electron transport from the donor to the acceptor side, n, is a function of light intensity and losses due to excitation quenching and fluorescence (see "Appendix"). When applied to PSII, charge recombination and reversal of the donor-side reduction are forbidden ($n' = j' = 0$), but these functions are active in PSI. Electron and proton transport by PQ is described by budget equations. The equation for electrons considers donation by PSII and cyclic electron transport (not activated in these calculations) and consumption by oxidation at Cyt b_6f. The oxidation rate is subject to photosynthetic control by proton back-pressure plus an allosteric function of the form of one- or two-proton equilibrium between the medium and the allosteric site. The budget equation for protons considers that $1H^+/e^-$ is donated by water splitting and $2H^+/e^-$ by PQ, assuming that the Q cycle is active. Considering that $4H^+/ATP$ are consumed, linear electron transport exactly satisfies the e^-/H^+ stoichiometry in photosynthesis, leaving no extra protons to generate the regulatory proton gradient and to compensate for leakage. These functions are fulfilled by pseudocyclic electron flow from the acceptor side of PSI, i.e. the Mehler-type O_2 reduction, and by the malate dehydrogenase-mediated shuttle of NADPH from the chloroplast to cytosol, where the reducing equivalents are oxidized by mitochondria. In the thylakoid protons are mostly bound to buffering structures. Free protons are consumed by ATP synthase and by leakage that is proportional to the concentration difference between the lumen and the stroma.

Fluorescence yields are calculated from the shallow-trap antenna-radical pair equilibrium model assuming that the quencher is activated only in the antenna. The primary radical pair $P680^+/Pheo^-$ is considered to be in equilibrium with the excitons in the antenna. Correspondingly, the antenna and the primary radical pair are considered together and the nonradiative decay from the antenna and from the primary radical pair state is described with the help of one rate constant for photochemical and one for nonphotochemical excitation quenching (the branched decay scheme in figure 2 of Lavergne and Trissl, 1995). The decrease of the redox potential of the primary radical pair in the state of singly reduced Q_a (van Mieghem et al., 1995) is not accounted for, and the rate constant for nonradiative decay is assumed to be independent of the reduction of Q_a (pure competition for excitation between the charge stabilization from $Pheo^-$ to Q_a, and nonphotochemical decay processes in the antenna and in the radical pair state). Fluorescence yields are calculated separately for closed and open PSII, and the steady-state fluorescence is the sum of the two. The nonphotochemically quenching sites are activated in a digital manner (yes/no), and the portion of activated quenchers is determined by protonation of the quenching sites in one-proton equilibrium. The protonation is fast, but the following conformational change in the antenna is slow.

Thus, the electron transport chain is modeled with two larger pools, PQ and NADPH, plus the pool of protons in thylakoids, for which the differential budget equations is numerically integrated. The portion of activated, nonphotochemically quenching sites, $N_{q'}$ is also described by a numerically integrated differential equation. Differential equations for photosystems (see "Appendix," Eqs. A1–A5) are solved analytically as quasi-stationary, expressing A, B, C, and D as functions of donor- and acceptor-side variables (PQ for PSII and PQ and NADPH for PSI) and light intensity. This allows lengthening of the numeric integration step, which is automatically controlled and varied from about 0.01 to 20 ms, depending on the stiffness of the situation.

Differential budget equations are also written for all intermediates of the Calvin cycle, Suc and starch synthesis pathways, considering maintenance of the phosphate pool in chloroplasts by the phosphate translocator and the control of Suc synthesis by Fru-2,6-bisP and starch synthesis by phosphoglyceric acid and other phosphates. Calvin-cycle enzymes are activated by electron pressure at the acceptor side of PSI and mediated by thioredoxin (for more details, see Laisk and Eichelmann, 1989; Laisk et al., 1989; Laisk and Walker, 1989; Laisk, 1993).

RESULTS

Interdependence between the Quantum Yields of Photochemical and Nonphotochemical Excitation Quenching

To compare the phenomenology of the stress-type q_I and rapidly reversible q_E, we related the Y_N (Eq. 5) to that of Y_P (Eq. 4) (Fig. 1). A general feature of these relationships is that when Y_P decreases, then Y_N increases in a rather complementary way, i.e. $Y_N + Y_P$ = constant = approximately 0.8 in a variety of treatments, including increasing light, decreasing CO_2 and O_2 concentrations, and also after thermoinhibition and photoinhibition. In some experiments in which F_{max} was not measured in the beginning of the experiment but only after the measurement of the light-response curve (transgenic tobacco, C_4 plants), dark F_o/F_m was less than 0.25, and $Y_N + Y_P$ was less than 0.8, but this did not alter the complementation.

However, the relationship was not always complementary, since in some sunflower and cotton leaves (grown at higher temperature or at low light) the increase in Y_N was less than the decrease in Y_P, although linearity was still maintained (data not shown). A less than complementary relationship between Y_N and Y_P was also obtained in sunflower after a long exposure to low light (PPFD of 220 μmol m^{-2} s^{-1} for several days) prior to photoinhibition (Fig. 1C, 0-h treatment). The calculation of Y_N and Y_P from F_m and F values measured in the dark during treatments with high temperature also shows a proportional but less than complementary relationship between the two quantum yields (white crosses on dark background, Fig. 1A). The same calculation with F and F_m measured in the dark after different degrees of photoinhibition reveals a complementary relationship, quite the same as typical for light mea-

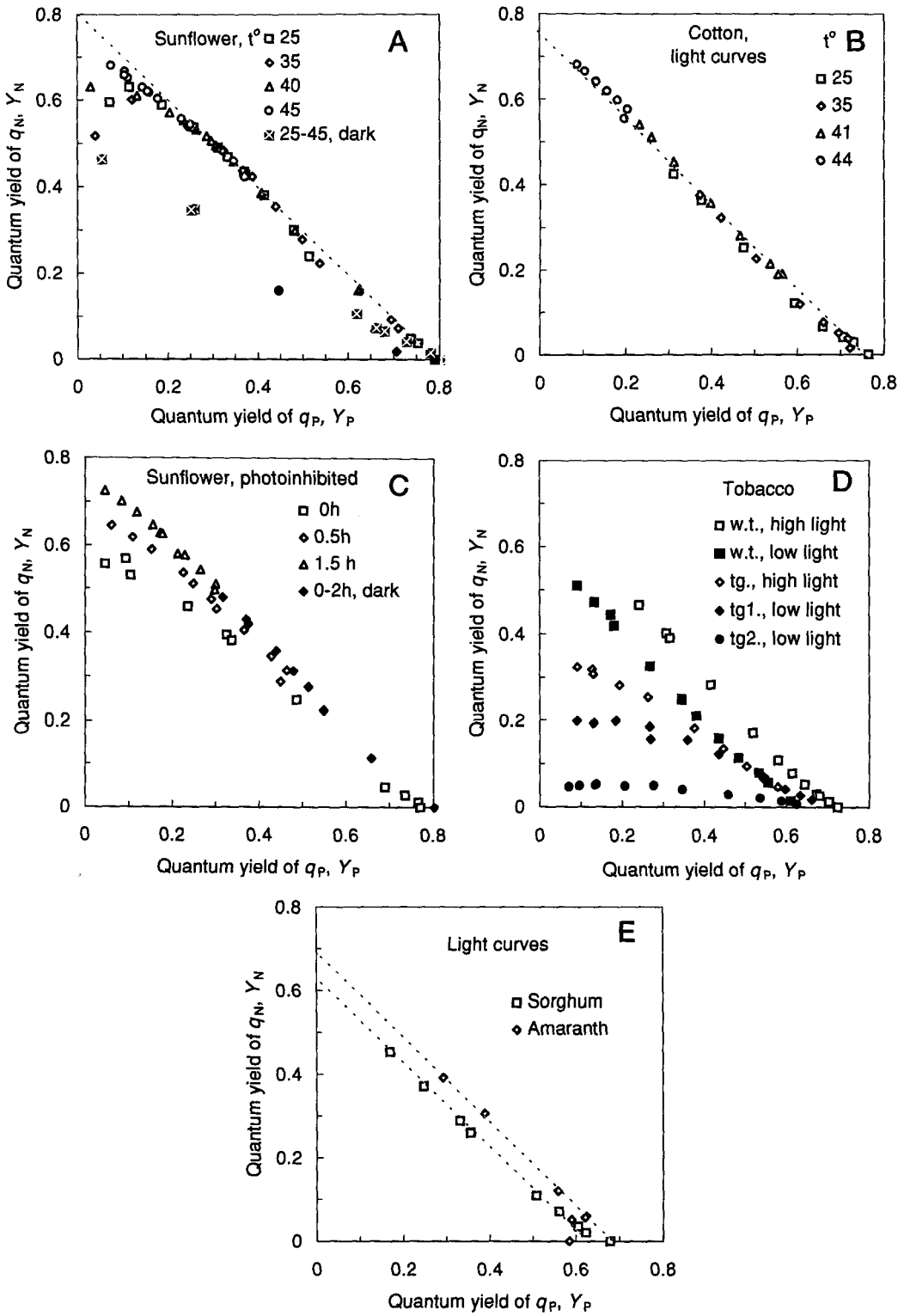

Figure 1. Interdependence between the quantum yields of photochemical (Y_P, Eq. 4) and nonphotochemical (Y_N, Eq. 5) excitation quenching in thermoinhibited sunflower grown at 18°C (A), in thermoinhibited cotton (B), in photoinhibited sunflower (C), in high-light-grown and low-light-grown wild-type (w.t.) and transgenic (tg.) Cyt b_6f-*deficient tobacco leaves (D), and in* C_4 plants sorghum and amaranth (E). Y_P was decreased by increasing light intensity and decreasing CO_2 concentration in 21 and 1.5% O_2 (A and C), by increasing light intensity at 330 μmol mol^{-1} CO_2 in 21% O_2 (B and E), or by increasing light intensity in 330 μmol mol^{-1} CO_2 and 1.5% O_2 (D). Filled symbols (A and C) were measurements in the dark; white crosses on dark background (A) were measured in the dark at increased temperatures. Filled diamonds (C) were measured in the dark after successively repeated photoinhibition for 15 min plus 15 min in the dark for each corresponding data point.

surements (filled diamonds in Fig. 1C). The linearity between Y_N and Y_P was lost when Y_P was severely suppressed by limiting electron transport with very low CO_2 and O_2 concentrations (left-most data points at lowest Y_P in Fig. 1, A and C), but not when electron transport rate was high and Y_P was suppressed by very high PPAD in the presence of electron transport (Fig. 1D, wild-type [w.t.] tobacco grown at low light).

Low values of Y_N and high values of Y_P could be recorded only in uninhibited leaves under low light. In the progress of thermoinhibition (Fig. 1, A and B) and photoinhibition (Fig. 1C), Y_N, was relatively high and Y_P was relatively low already in the dark (filled data points in Fig. 1A) and at low light intensities, and Y_P decreased further when light intensity was increased and CO_2 concentration was decreased. At 45°C there was a considerable portion of thermoinhibited PSII centers, but the maximally quenched F'_m was exactly the same as at 25°C when there was no irreversible inhibitory quenching. In the Cyt b_6f-deficient transgenic tobacco Y_N stopped increasing at a rather low ceiling, although Y_P continued to decrease. This ceiling was different in different leaves, probably a function of the degree of the expression of the Rieske protein in these transgenic plants. In the C_4 plants sorghum and amaranth, the relationship between Y_N and Y_P was exactly complementary at higher PPADs, but these two plants showed interesting opposite behavior at low PPADs. In sorghum, the steady-state F' slightly increased; in amaranth, it decreased at low PPADs and then stayed constant. In Y_N versus Y_P axes this is transformed into a decrease in Y_P without a sufficient increase in Y_N for sorghum, and an increase in Y_N without a decrease in Y_P for amaranth.

Interdependence between the Rate Constants for Photochemical and Nonphotochemical Excitation Quenching

The average rate constant k'_P was calculated from Equation 7, k'_{PO} was calculated from Equation 8, and the rate constant k'_N was calculated from Equation 6. The plot of k'_N versus k'_P represents in a more sensitive way the relationship between changes in q_P and q_N than the plot of Y_N versus Y_P, since in cases in which a deviation from complementation occurs, both numerator and denominator change in Equations 4 and 5. The average rate constant k'_P decreases as a result of the PSII acceptor-side closure, and k'_N concomitantly increases (Fig. 2). In normally developed leaves, k'_N and k'_P were also complementary within a certain range, but usually the relationship was somewhat sigmoidal: k'_N increased little in response to some initial decrease in k'_P and then became complementary (Fig. 2, A and C). Only in amaranth did k'_P increase at low PPADs before the complementary relationship was established at saturating PPADs. The increase of k'_N was less than complementary in leaves exposed to low light before photoinhibition experiments (Fig. 2B), and in the Cyt b_6f-deficient tobacco k'_N increased only to a certain ceiling (Fig. 2C). It was expected that k'_{PO} would not change while k'_N was increasing, but it did. In all experiments k'_{PO} decreased with increasing k'_N, but with the rate of about one-half of that of k'_P (Fig. 2, C and D; in other figs. not shown but similar). This decrease of k'_{PO} was caused by a smaller relative decrease in F'_o than expected from Equation 1 with increasing k'_N. The relative quenching of F'_o could be enhanced by subtracting (0.3–0.5) F_o from all F' values since the pulse-amplitude-modulated fluorometer is reported to be sensitive to the small constant fluorescence of PSI (Genty et al., 1990). As a result, k'_{PO} could be made closer to constant with increasing k'_N, in agreement with the notion that nonphotochemical quenching is competitive for the photochemical quenching in an open reaction center (data not shown).

Numeric Experiments with the Model

The system of differential equations (see "Appendix") was integrated using Euler's method (Iserles, 1996). Steady-state results were obtained by waiting until transient processes were completed after light intensity was changed. The steady-state light-response curves of photosynthetic O_2 evolution rate and fluorescence parameters were calculated for a CO_2-limited case (5 μM at the Rubisco sites) under nonphotorespiratory conditions (Fig. 3). F'_m did not reach the maximum of 1.0 even at the lowest PPAD of 20 μmol m^{-2} s^{-1} because some ΔpH was always necessary to drive photosynthesis and the corresponding drop in lumen pH caused an initial small q_N. This initial q_N could be changed by changing pK_{50} (set to 5.2) of the deprotonation of the quenching sites. F'_m slightly decreased while photosynthesis was lightlimited, but abruptly dropped when light saturation was reached. This happened because lumen pH slowly decreased while photosynthesis was light limited but rapidly decreased around the inflection point of the light-response curve of photosynthesis to saturation. The speed of saturation of the light response depended on the redox potential difference between PQ and PS1D (PSI donor side). The midpoint redox potential value for PQ, E_{PQ}, was set to +0.117 V, and the results in Figure 3 were calculated with the midpoint redox potential of E_{PS1D} = +0.15 V. The higher the E_{PS1D}, the sharper the inflection to saturation, the larger the drop of F'_m immediately at the inflection, and the less efficient the photosynthetic control by proton back-pressure at Cyt b_6f. F'_m continued to decrease under light saturation because lumen pH continued to decrease due to the alternative electron transport via the Mehler reaction from the acceptor side of PSI. Steady-state F' slightly increased during the light-limited part of the response, but dropped again under light saturation, varying only a little over the whole light curve.

Data from Figure 3 and other calculations are presented as quantum yields and relative rate constants for excitation quenching in Figure 4. There is approximate complementation between Y_N and Y_P when $k'_{Nm} = k'_P$, which was the obligatory condition for the complementation. When k'_P = 4 and k'_{Nm} = 2, Y_N did not extrapolate to the maximum, equal to the maximum of Y_P (Fig. 4, diamonds). As in experimental results, Y_N increased less than Y_P decreased at low light intensities (high Y_P values), causing a slight concavity of the Y_N versus Y_P dependence. This concavity was caused by a buildup of electron pressure at the PSII

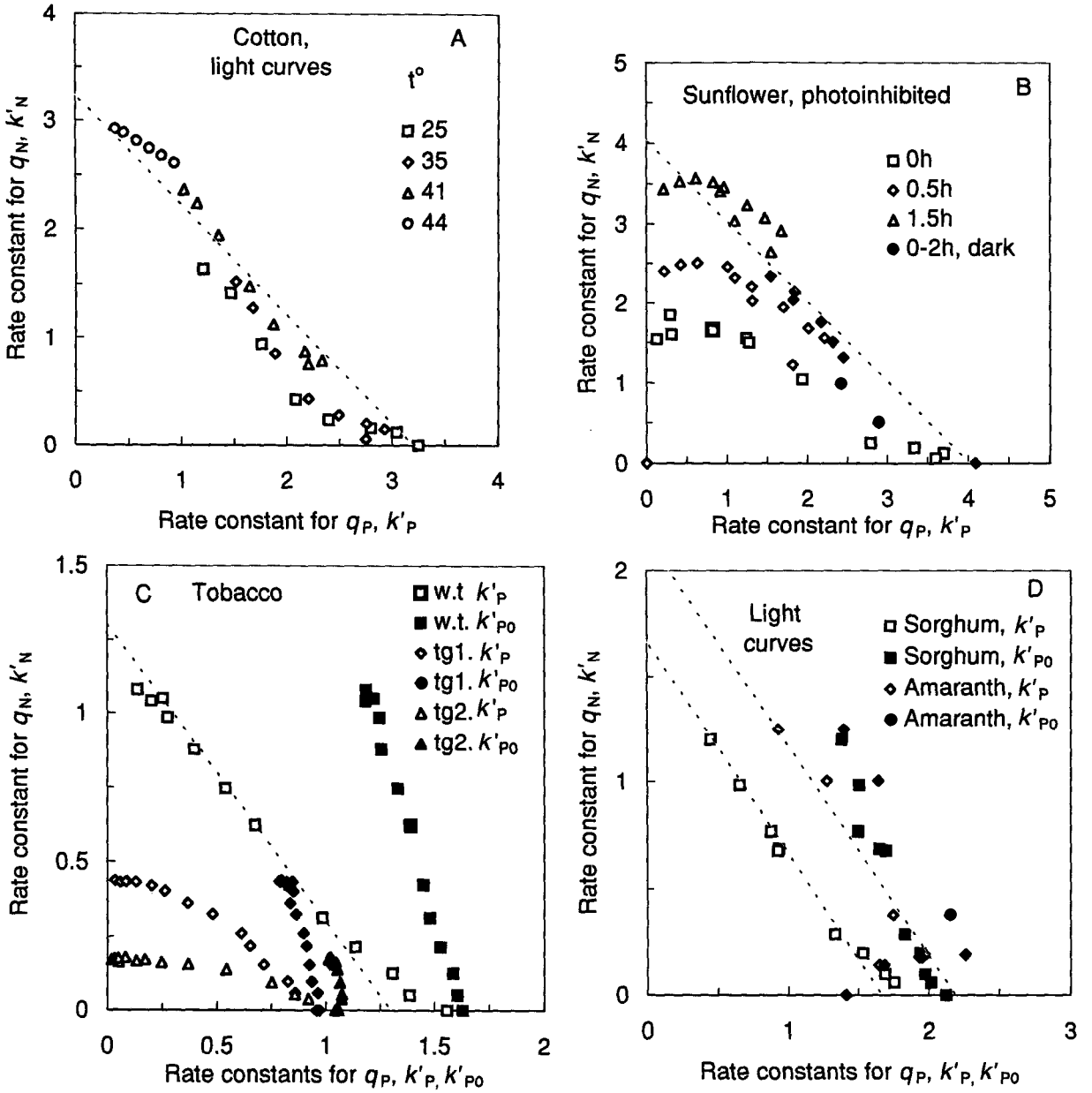

Figure 2. Interdependence between the relative rate constant for nonphotochemical excitation quenching (k'_N, Eq. 6) and the average rate constant for photochemical excitation quenching (k'_P, Eq. 7) and the photochemical rate constant for open centers (k'_{PO}, Eq. 8; filled symbols, only in C and D) in thermoinhibited cotton (A; data from Fig. 1B), in photoinhibited sunflower (B; data from Fig. 1C), in wild-type (w.t.) and transgenic (tg.) tobacco (C; data from Fig. 1D), and in the C_4 plants (D; data from Fig. 1E).

acceptor side under light limitation and was sensitive to the rate of electron transfer from PSII to PQ. When V_{m45} was decreased from 2 to 1 M s^{-1}, the concavity increased (Fig. 4, triangles).

The same results are presented as relative rate constants k'_P and k'_N in Figure 4B. In this presentation it is clearly visible that the dependence of k'_N on k'_P is not a straight line but sigmoidal, a reflection of the slow decrease in thylakoid pH at low PPADs and of the saturating protonation equilibrium of the quenching sites (see "Appendix," Eq. A20) at low thylakoid pH. When pK_{50} for the protonation of the quenching sites was increased from 5.2 to 5.7, there was more nonphotochemical quenching at low PPADs and the maximum possible k'_N of 4 was closely reached at the high PPADs (Fig. 4, crosses). The sigmoidicity of the k'_N versus k'_P dependence increased when biproton equilibrium was assumed in Equation A20 (see "Appendix") for the protonation of the quenching sites (data not shown). For all cases the modeled k'_{PO} versus k'_N plots were vertical, i.e. k'_{PO} did not change when k'_N increased, as expected from the competition between q_P and q_N centers for excitation in the same antenna.

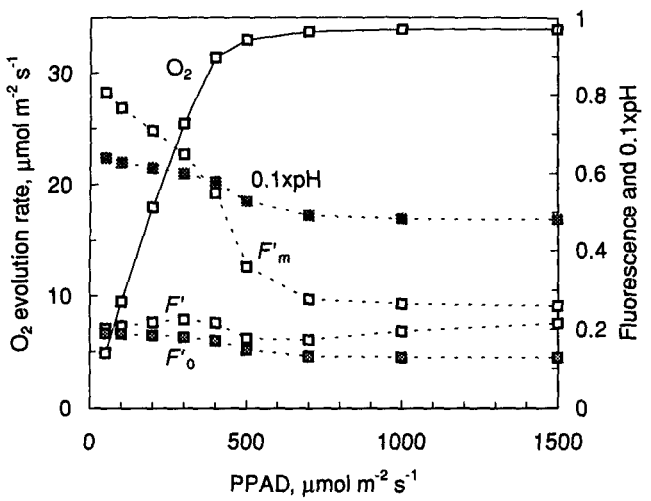

Figure 3. Modeled light-response curves of O_2 evolution (solid line, left ordinate), and fluorescence yields F' (steady-state), F'_m (pulse-saturated), and F'_0 (dark) and lumen pH (dotted lines, right ordinate). Model was under nonphotorespiratory conditions using parameters given in the "Appendix."

DISCUSSION

Approximate complementation between the quantum yields of nonphotochemical and photochemical excitation quenching has been found in *Lamium galeobdolon* leaves exposed to different light intensities (Genty et al., 1996). Our work shows that this approximately complementary interdependence of the two quantum yields is a rather universal phenomenon, independent of the way the photochemical yield was changed and quite the same for the rapidly reversible q_E and for q_I. From the complementation between the quantum yields of photochemical and nonphotochemical quenching, it follows that the sum of the two is constant (about 0.8 in most leaves):

$$Y_P + Y_N = \frac{k'_P + k'_N}{1 + k'_P + k'_N} = 0.8 \quad (9)$$

from which

$$k'_P + k'_N = 4 \quad (10)$$

Equation 10 shows that the complementation of the quantum yields also means the complementation of the rate constants (in experiments in which $k'_P + k'_N < 4$ [Fig. 2, C and D], F_{max} probably did not reach the absolute maximum because of short dark exposure). However, because of the competitiveness between photochemical and nonphotochemical excitation decay, Y_N always increases when Y_P decreases, even when k_N stays constant. Thus, although the presentation of the quantum yields Y_N and Y_P illustrates how well nonphotochemical quenching substitutes for photochemical quenching, it is not sensitive enough to investigate correlated variations in k'_P and k'_N. Small deviations from the complementation of the quantum yields (Figs. 1 and 4A) represent big deviations from the complementation of the rate constants (Figs. 2 and 4B). For example, in most of our experiments at low light intensities k'_N tended to increase less than k'_P decreased (sigmoidicity), which reflects the buildup of the necessary electron pressure to drive electron transport (Q_a reduction), accompanied by less than a complementary increase in the nonphotochemical quenching due to a relatively slowly decreasing thylakoid pH. This phase of the buildup of electron pressure is also well reproduced, as shown in Figure 4B, which shows that the initial sigmoidicity depends on the rate constant for PQ reduction by PSII. An exception was amaranth, in which k'_N increased without a decrease in k'_P at low light (Figs. 1E and 2D). Possibly, in this plant Q_a was somewhat reduced in the dark by internal reductants and became more oxidized at low light when PSI was activated.

In the Stern-Volmer formulation k'_P is an average over a part of open reaction centers and the complementary part of closed centers; therefore, its decrease is mainly caused by increasing the number of closed reaction centers. Thus, data in Figures 1 and 2 present a positive relationship between the PSII acceptor-side closure and nonphotochemical excitation quenching. However, it has been proven that at least the q_E quenching is not directly related to the reduction of Q_a but is induced by low thylakoid pH, and neither the active PSII, the S-state transitions, nor a cycle around PSII are required for q_E quenching (Crofts and Yerkes, 1994). To explain the relationship between the Q_a reduction and q_E quenching, the low thylakoid pH (which induces q_E quenching) and Q_a reduction must be correlated. Such correlation is expected because high ΔpH is generated when ATP consumption is limited and Q_a becomes highly reduced when electron acceptors are limiting. In general, the decrease in photochemical excitation quenching reflects the back-pressure of electrons; the increase in nonphotochemical excitation quenching reflects the back-pressure of protons. However, it is not obvious that the pH dependence of the process must be such that the resulting increase in the nonphotochemical quenching constant must be complementary to the decrease in the photochemical quenching constant. In the numeric experiments with the model, only sigmoidal interdependencies between k'_N and k'_P were obtained (Fig. 4B), which reflected the assumed one-proton equilibrium at the quenching sites (the sigmoidicity was enhanced when biproton equilibrium was assumed). Such sigmoidicity qualitatively agreed with some experiments (Fig. 2, A and B), but not with others (Fig. 2C, w.t. tobacco; Fig. 2D). A complex equilibrium condition for the protonation of the quenching sites may be postulated that will produce nearly linear dependence between k'_N and k'_P, but it seems to be a formal solution to the problem.

The approximate complementation between k'_N and k'_P would also be possible to explain if the PQ and proton pools were not bulk pools, but rather were restricted to the neighborhood of individual PSII complexes, or at least if they formed domains that accommodate many interconnected PSII and Cyt b_6f, but no connection is allowed between the domains. In this case it is only necessary that complete PQ reduction (resulting in Q_a reduction) and maximum proton gradient (resulting in complete nonphotochemical quenching) would occur simultaneously in

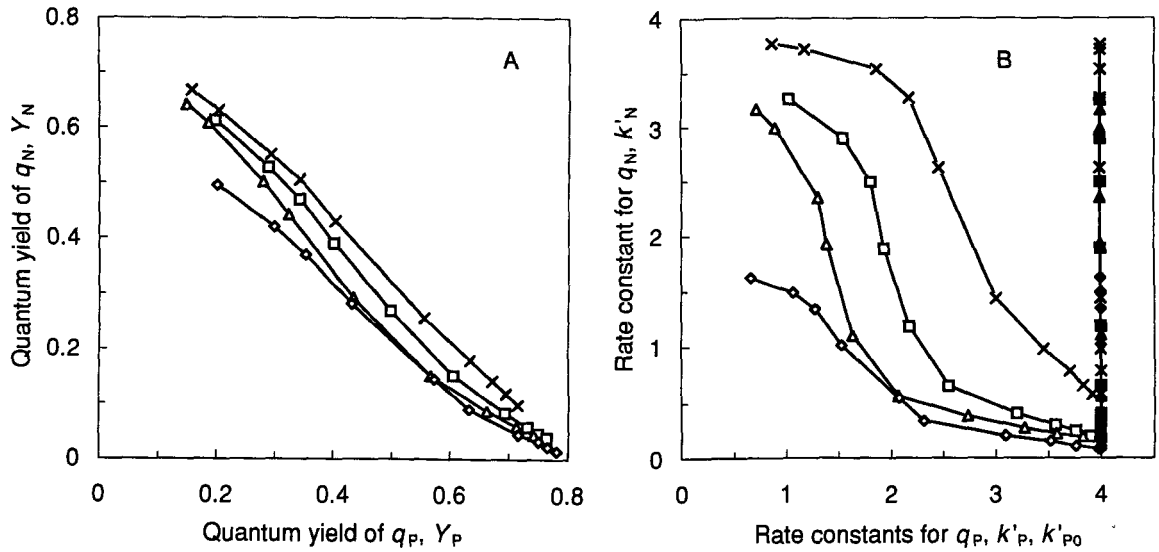

Figure 4. Interdependence between Y_P and Y_N calculated from numeric experiments (A). Squares, Data from Figure 3; diamonds, same as squares but k_{Nm} changed from 4 to 2; triangles, same as squares but V_{m45} changed from 2 to 1 M s^{-1}; crosses, same as squares but pK_{50} changed from 5.2 to 5.7. B, Interdependence between the rate constant for k'_N and the average rate constant for k'_P (open symbols), and the photochemical rate constant for k'_{PO} (closed symbols) using data from A.

those domains. This condition is rather likely to be filled because PQ reduction is the result of a strong photosynthetic control of its oxidation rate at Cyt b_6f caused by high proton gradient. The driving force for transmembrane proton translocation is strongest when PQ reduction is at a maximum. Kinetic evidence that PSII and Cyt b_6f are complexed in a way that cross-diffusion of PQ between the domains is restricted (Joliot et al., 1992, 1993; Andree et al., 1995) supports our model. Actually, it is not even necessary that PSII and Cyt b_6f form pairs. Rather, big domains, e.g. single thylakoids, are allowed if nonphotochemical quenching is regulated by luminal pH simultaneously for all PSII in the thylakoid. If the most acidic pH is achieved at different threshold light intensities in different thylakoids (e.g. because of gradients inside the leaf), the sigmoidal functions of single thylakoids are shifted with respect to each other and the sigmoidicity of the response will be smoothed. Our mathematical model is based on the assumption of bulk pools of PQ, protons, and NADPH and uniform external conditions (CO_2 and light) and cannot mimic such compartmented photosynthesis. Thus, the discrepancies between model simulations and experimental results may point to structural differences that lead to different kinetic behavior.

In the numeric experiments maximum k'_P and maximum k'_N were equal only if so postulated ($k'_{Nm} = k'_P = 4$), but not when $k'_{Nm} = 2$. Data obtained with the Cyt b_6f-deficient tobacco showed a similar behavior (Fig. 2C): in these leaves q_E quenching developed with a rather normal speed at low light intensities, but then it reached a ceiling, probably because luminal pH did not decrease subsequently. In normally developed leaves, usually $k_{Nm} = k'_P$ (= approximately 4), for which a mechanistic reason is expected. For example, the condition that $k'_{Nm} = k'_P$ is expected if a photochemically active and highly fluorescent center changes into a nonfluorescent and photochemically less active state (Weis and Berry, 1987; Krieger and Weis, 1992, 1993), maintaining the same rate constant of excitation capture as the fluorescent state. Such a center-quenching mechanism, based on the slow water splitting that creates oxidized sites on the donor side and facilitates back-reaction from the acceptor side of PSII, is generally believed to be the basis for inhibitory quenchings (Schreiber and Neubauer, 1987, 1990; Prasil et al., 1992; Havaux, 1993), and was originally proposed also for the q_E-type reversible quenching (Weis and Berry, 1987). From this aspect it is noteworthy that the same interdependence between the quantum yields and rate constants of photochemical and nonphotochemical quenching was observed in our experiments whether the quenching was q_E or q_I (e.g. measurements in the dark after progressive photoinhibition; Figs. 1C and 2B), which points to the possible similarity in the mechanisms of q_E and q_I.

As an alternative explanation, in photoinhibited (maybe also in thermoinhibited) leaves the persistent quenching might be caused by a kind of long-lived q_E-type antenna quenching caused by zeaxanthin and low pH induced by ATP hydrolysis in the dark (Gilmore and Björkman, 1994a, 1994b) or chlororespiration (Ting and Owens, 1993), which may stay even after ΔpH has relaxed (Ting and Owens, 1994). However, if one assumes that the dark ΔpH is the cause of the inhibitory quenching, it is difficult to explain the closely complementary relationship between k'_P and k'_N in the dark (Fig. 2B), which would mean a similarly close relationship between ΔpH and Q_a reduction as discussed above, but in the dark.

Although the center-quenching model better explains the complementation between photochemical and nonphoto-

chemical excitation quenching, it is unable to explain the role of zeaxanthin in quenching, which is located in the antenna, and several other kinetic phenomena (Horton and Ruban, 1994; Ting and Owens, 1994). A proposed mechanism of antenna quenching explains q_E as excitation quenching in the minor CP24 and CP29 complexes of the antenna caused by too close an interaction between chlorophylls that are displaced as a result of ligand protonation (Crofts and Yerkes, 1994). Also, zeaxanthin may be conformationally moved into contact with chlorophylls when proteins are protonated (Horton and Ruban, 1994; Horton et al., 1994, 1996; Owens, 1994). In our mathematical model this protonation was assumed to be fast but the conformational change slow (see "Appendix," Eqs. A20 and A21). Development of nonphotochemical quenching in antenna must cause no change in the rate constant k'_{PO}. This was confirmed in the model calculations (Fig. 4B). In all experiments k'_{PO} did not stay constant but decreased when k'_N increased (Fig. 2, C and D). The reason for this was relatively less quenching of F'_o than expected from the competitive antenna quenching. There is the possibility that the F'_o quenching might be curtailed by a simultaneous increase in F'_o caused by permanent reduction of Q_a at a small fraction of PSII, which is very likely under inhibitory conditions, and the possibility that a part of F'_o, as measured by the pulse-amplitude-modulated fluorometer, may come from PSI (Genty et al., 1990). Therefore, we cannot state for sure that the actual quenching of F'_o in open centers really was smaller than predicted by the monopartite antenna quenching model.

In summary, our experimental results show an approximately complementary relationship between the quantum yields of nonphotochemical and photochemical excitation quenching under energized and inhibitory conditions. Much of that complementation is the result of competition between the photochemical and nonphotochemical ways of excitation quenching, but expression of the results as relative rate constants shows a correlated increase in k'_N with a decrease in k'_P, which are rather closely complementary in some experiments.

The parallel development of Q_a reduction (which causes the decrease in k'_P) and transmembrane ΔpH (which causes the increase in k'_N) could be quantitatively explained by the present knowledge of photosynthesis, organized in a mathematical model. Thermodynamically, the model represents photosynthesis as driven by downhill flow of protons and electrons. Under rate-limiting conditions downstream, the pressure of electrons causes decreased photochemical excitation quenching, and the pressure of protons causes increased nonphotochemical excitation quenching. The complementation of the two types of quenching indicates a good balancing of electron and proton pressures. Complete complementation of the two types of quenching was not achieved with the functions used in the model. Differences between experimental results and model simulations may be explained assuming that electron transport is organized in domains that contain relatively complete electron and proton transport chains. This may be the reflection at the leaf level of the organization of the photosynthetic machinery in thylakoids. Whether in bulk or in domains, the complementation of the rate constants for photochemical and nonphotochemical quenching ensures that the steady-state fluorescence yield in the light F' stays close to the dark-adapted F_o. This guarantees that the average lifetime of excitation stays constantly at a minimum, whether or not photochemistry is possible. Minimal lifetimes of excitation help to avoid the formation of triplet-state chlorophylls, production of reactive oxygen species, and radicals. It is logical that as the capacity for photochemical quenching decreases, that of nonphotochemical quenching increases to minimize damage due to singlet oxygen or photoinhibition. But it must not increase more than the decrease in photochemical quenching, or too large a fraction of the excited states would be dissipated. Selection of organisms with a precise (complementary) control between the two forms of quenching could be expected on an evolutionary time scale.

APPENDIX

Mathematical Model

PSII and PSI have donor (D) and acceptor (A) side carriers that can be reduced or oxidized. As a result, each of the photosystems is a sum of the following partial states: $A = D^-A^-$; $B = D^-A^+$; $C = D^+A^-$; $D = D^+A^+$. PSII and interphotosystem electron transport are described by the following system of differential equations:

$$\frac{dA}{dt} = -(j' + q)A + q'B + jC = 0 \quad \text{(A1)}$$

$$\frac{dB}{dt} = qA - (j' + q' + n)B + n'C + jD = 0 \quad \text{(A2)}$$

$$\frac{dC}{dt} = j'A + nB - (q + j + n')C + q'D = 0 \quad \text{(A3)}$$

$$\frac{dD}{dt} = j'B + qC - (j + q')D = 0 \quad \text{(A3)}$$

$$A + B + C + D = PS2T \quad \text{(A5)}$$

$$\frac{dPQ^-}{dt} = \frac{V_{45} - V_{42} + V_{46}}{2} \quad \text{(A6)}$$

$$\frac{dHI_t}{dt} = \frac{V_{memb}(V_{45} + HER \times V_{42}) - V_{str} \times HPR \times V_{12}}{V_{thyl}} - V_{44} \quad \text{(A7)}$$

where $PS2T$ is the total of PSII and the rate constants are j for donor-side reduction, n for donor-acceptor transport, and q for acceptor-side oxidation. Rate constants for reverse reactions are supplied by primes. PQ^- is reduced PQ and HI_t stands for free plus bound hydrogen ions in thylakoid lumen. Reaction rates are V with subscript reaction numbers: 45 for PQ reduction by PSII acceptor side; 42 for plastoquinol oxidation by PSI via the Cyt b_6f complex; 46 for cyclic electron flow from PSI acceptor side (not activated in these calculations); 44 for proton leak; and 12 for ATP synthase. Instead of cyclic electron flow, electron pressure at the acceptor side of PSI is released by activating

NADP-malate dehydrogenase and shuttling reducing equivalents out of the chloroplast, and by introducing an alternative electron flow away from the PSI acceptor side as the Mehler reaction (equations not shown here). *HER* is proton/electron ratio for plastoquinol oxidation; *HER* = 2 when the Q cycle is active. *HPR* (=4) is the proton/phosphate ratio for ATP synthase. V_{memb}, V_{thyl}, and V_{str} denote the volumes of thylakoid membrane, thylakoid lumen, and stroma, respectively: $Chl = 3.89 \times 10^{-4}$ mol m^{-2}, $V_{memb} = 2.25 \times Chl$, L m^{-2}, $V_{thyl} = 1.0 \times V_{memb}$, and $V_{str} = 10 \times V_{memb}$.

Constants in Equations A1 to A7 are related to leaf parameters as follows. The total number of PSII centers,

$$PS2T = \frac{Chl2}{PSU2 \times V_{memb}} \tag{A8}$$

where $PS2T$ is expressed in mol L^{-1} in thylakoid membrane volume, $Chl2$ is the molar amount of chlorophyll around PSII (in calculations, 0.45 of the total), $PSU2$ is the photosynthetic unit of PSII (200 Chl). The fraction of PSII with reduced acceptor-side $PS2Q^- = A + C$ and that with oxidized acceptor-side $PS2Q = B + D = PS2T - PS2Q^-$.

Excitation rate (ER_{Chl2}) per chlorophyll s^{-1} depends on the PPAD:

$$ER_{Chl2} = \frac{PPAD}{Chl} \tag{A9}$$

(for PSI additional far-red excitation is allowed). The rate constant n for electron transport from the donor to the acceptor side of PSII is dependent on the excitation rate of PSII chlorophyll, considering losses for fluorescence and nonradiative decay:

$$n = PSU2 \times ER_{Chl2} \times \frac{k'_P}{1 + k'_P + k'_N} \tag{A10}$$

where k'_P is the effective rate constant for charge stabilization and k'_N is that for nonphotochemical excitation quenching (rate constants k' have the same relative meaning as in Eq. 1). Donor-side rate constant j is preset fast for PSII, but it is photosynthetically controlled by Cyt b_6f and ΔpH for PSI. Electron transport rate from PSII acceptor side to PQ is expressed as follows:

$$V_{45} = \frac{V_{m45}(PS2Q^- \times PQ - PS2Q \times PQ^-/kE_{45})}{PS2T \times K_{m45PQ}\left(1 + \frac{PQ}{K_{m45PQ}} + \frac{PQ^-}{K_{m45PQ^-}}\right)} \tag{A11}$$

$$PQ = PQT - PQ^- \tag{A12}$$

where V_{m45} is the maximum turnover rate of the reaction, PQT is the total concentration of PQ, PQ and PQ^- are the concentrations of oxidized and reduced PQ in the membrane, subscripts at K_m indicate the substrate form, and kE_{45} is the equilibrium constant calculated from the difference of redox potentials as described by Laisk and Walker (1989). Accordingly, the PSII acceptor-side rate constants of electron transfer are the following:

$$q = \frac{V_{m45} \times PQ}{PS2T \times K_{m45PQ}\left(1 + \frac{PQ}{K_{m45PQ}} + \frac{PQ^-}{K_{m45PQ^-}}\right)} \tag{A13}$$

and

$$q' = \frac{V_{m45} \times PQ^-/kE_{45}}{PS2T \times K_{m45PQ}\left(1 + \frac{PQ}{K_{m45PQ}} + \frac{PQ^-}{K_{m45PQ^-}}\right)} \tag{A14}$$

Fluorescence yields are calculated as follows. For open PSII centers:

$$F'_o = \frac{1}{1 + k'_P + k'_N}. \tag{A15}$$

For closed PSII centers:

$$F'_m = \frac{1}{1 + k'_N}. \tag{A16}$$

For the mixture of closed and open centers in the steady state:

$$F' = \frac{F'_o \times PS2Q + F'_m \times PS2Q^-}{PS2T} \tag{A17}$$

In Equations A15 to A17, we have assumed that $k_f = 1$ and neglected the thermal decay k_d, a nonphysical assumption, but it allows one to scale the fluorescence to $F_{max} = 1$. The rate of plastoquinol oxidation by the Cyt b_6f complex:

$$V_{42} = V_{m42} \times CF_{42} \times \frac{[PQ^- \times PS1D - PQ \times PS1D^-/(kE_{42} \times HI_{fs}/HI_{ft})]}{PS1T \times K_{m42PQ^-}\left(1 + \frac{PQ^-}{K_{m42PQ^-}} + \frac{PQ}{K_{m42PQ}}\right)} \tag{A18}$$

where CF_{42} is a photosynthetic control factor:

$$CF_{42} = \frac{1}{1 + \left(\frac{HI_{ft}}{K_{i42}}\right)^2} \tag{A19}$$

Photosynthetic control of plastoquinol oxidation is executed by proton back-pressure, which shifts the equilibrium in Equation A18 (Because of obligatory Q-cycle $2H^+/e$ are transported in reaction 42, consequently, the ratio of proton concentrations must be in square [Dave Kramer, personal communication].) and/or by a regulatory control factor CF_{42}, which is activated by one- or two-proton equilibrium between the catalytic site and free protons (in calculations in this work, only proton back-pressure was controlling the electron flow). Similarly to Equations A13 and A14, the first and second term of Equation A18 form the donor-side forward and reverse rate constants for PSI. At the acceptor side of PSI NADPH is assumed to form a free pool, mathematically treated like PQ at PSII. Calvin-cycle enzymes are activated by electron

pressure at the acceptor side of PSI, mediated by thioredoxin.

Along with the transport of each electron, three protons are accumulated in the thylakoid lumen, one at PSII and two at Cyt b_6f, with the help of the active Q cycle. The concentration of free protons in the thylakoid HI_{ft} is calculated using buffer equations (Laisk and Eichelmann, 1989; Laisk and Walker, 1989). Accumulated protons are consumed for ATP synthesis (four per ATP) and can leak out proportionally with the concentration difference. Free protons in the thylakoid immediately protonate quenching sites QH, which is modeled by a single-proton equilibrium with an equilibrium constant kE_{50} calculated from the preset pK_{50}:

$$QH = \frac{(HI_{ft}/kE_{50})}{1 + (HI_{ft}/kE_{50})} \quad \text{(A20)}$$

The rate constant of nonphotochemical excitation quenching k'_N is calculated from a differential equation that considers the relatively slow conformational change of the quenching sites:

$$\frac{dk'_N}{dt} = RC_{50} \times (QH \times k'_{Nm} - k'_N) \quad \text{(A21)}$$

where k'_{Nm} is the maximum possible k'_N and RC_{50} determines the rate of equilibration. Equation A21 describes an exponential approach of k'_N to the level $QH \times k'_{Nm}$, where QH varies from 0 to 1.

Some parameter values used in the calculations: CO_2 concentration, 5 μM at the carboxylation sites (usual in C_3 plants at the external atmospheric CO_2 concentration); midpoint redox potentials: PSII acceptor quinone, −0.24 V; PQ, +0.117 V (the difference is set to ensure fast electron flow from Q_a to PQ and to correctly simulate light-dark transients in fluorescence); PSI donor side, +0.15 V (set lower than usual to ensure photosynthetic control at Cyt b_6f by proton back-pressure; this value may be increased when the ratio of proton concentrations is in square in Eq. A18); PQT = 7 mM in the membrane (compares with measured PQ pools; Laisk et al., 1992); V_{m42} = 1 M s^{-1} (ensures adequate steady-state rate in the presence of proton gradient); K_{m42PQ^-} = 0.1 mM (makes PQ^- oxidation rate largely independent of PQ^- concentration); pK_{42} = 4.5 (set low to switch off allosteric control of electron transport through Cyt b_6f); V_{m45} = 2 M s^{-1} (ensures maximum PSII electron transport rate about five times faster than necessary for steady-state photosynthesis; Laisk et al., 1992); K_{m45PQ} = 1 mM (makes PQ reduction rate largely independent of PQ concentration; Laisk et al., 1992); pK_{50} = 5.2 (ensures the wide range of q_E change in dark-light transients and small q_E at very low PPADs); RC_{50} = 0.1 s^{-1} (sets the relaxation rate for q_E); k_f = 1 (relative unity); k_d = 0 (not important in relative scale if k_f = 1 and k_N is present); k'_P = 4 (ensures realistic quantum yield of photosynthesis and the correct F_v/F_m ratio); k'_{Nm} = 4 (ensures complementation between q_N and q_P); $j = 1 \times 10^6$ (ensures fast re-reduction of PSII donor side); $j' = n' = 0$ (no charge recombination from Q_a, no reversal of donor side reduction); pH_s = 8.04 (in stroma).

ACKNOWLEDGMENTS

The seeds of the Cyt b_6f-deficient transgenic tobacco were kindly provided by G.D. Price (R.S.B.S., Australian National University, Canberra). G. Edwards' reading of the manuscript and comments by an unknown reviewer are highly appreciated.

Received January 13, 1997; accepted July 4, 1997.
Copyright Clearance Center: 0032–0889/97/115/0803/13.

LITERATURE CITED

Andree S, Spittel M, Weis E (1995) Distribution, organisation and functional state of PS I, PS II and LHC-complexes in thylakoids after LHCII phosphorylation. *In* P Mathis, ed, Photosynthesis: From Light to Biosphere, Vol III. Kluwer Academic Publishers, Dordrecht, The Netherlands, pp 233–236

Crofts AR, Yerkes CT (1994) A molecular mechanism for qE-quenching. FEBS Lett **352:** 265–270

Dainese P, Santini C, Chiretti-Magaldi A, Marquardt J, Tidu V, Mauro S, Bergantino E, Bassi R (1992) The organization of pigment-proteins within photosystem II. *In* N Murata, ed, Research in Photosynthesis, Vol II. Kluwer Academic Publishers, Dordrecht, The Netherlands, pp 13–20

Foyer C, Furbank R, Harbinson J, Horton P (1990) The mechanisms contributing to photosynthetic control of electron transport by carbon assimilation in leaves. Photosynth Res **25:** 83–100

Genty B, Briantais JM, Baker NR (1989) The relationship between quantum yield of photosynthetic electron transport and quenching of chlorophyll fluorescence. Biochim Biophys Acta **990:** 87–92

Genty B, Harbinson J, Cailly AL, Rizza F (1996) Fate of excitation at PS II in leaves: the nonphotochemical side. Presented at The Third BBSRC Robert Hill Symposium on Photosynthesis, March 31 to April 3, 1996, University of Sheffield, Department of Molecular Biology and Biotechnology, Western Bank, Sheffield, UK, abstract no. P28

Genty B, Wonders J, Baker NR (1990) Non-photochemical quenching of F_o in leaves is emission wavelength dependent: consequences for quenching analysis and its interpretation. Photosynth Res **26:** 133–139

Gilmore AM, Björkman O (1994a) Adenine nucleotides and the xanthophyll cycle in leaves. I. Effects of CO_2- and temperature-limited photosynthesis on adenylate energy charge and violaxanthin de-epoxidation. Planta **192:** 526–536

Gilmore AM, Björkman O (1994b) Adenine nucleotides and the xanthophyll cycle in leaves. II. Comparison of the effects of CO_2- and temperature-limited photosynthesis on photosystem II fluorescence quenching, the adenylate energy charge and violaxanthin de-epoxidation in cotton. Planta **192:** 537–544

Green BR, Durnford DG (1996) The chlorophyll-carotenoid proteins of oxygenic photosynthesis. Annu Rev Plant Physiol Plant Mol Biol **47:** 685–714

Havaux M (1993) Characterization of thermal damage to the photosynthetic electron transport system in potato leaves. Plant Sci **94:** 19–33

Horton P, Oxborough K, Rees D, Scholes JD (1988) Regulation of the photochemical efficiency of photosystem II: consequences for the light response of field photosynthesis. Plant Physiol Biochem **26:** 453–460

Horton P, Ruban A (1994) The role of light harvesting complex II in energy quenching. *In* NR Baker, JR Bowyer, eds, Photoinhibition of Photosynthesis from Molecular Mechanisms to the Field. BIOS Scientific Publishers, Oxford, UK, pp 111–142

Horton P, Ruban AV, Walters RG (1994) Regulation of light harvesting in green plants. Plant Physiol **106:** 415–420

Horton P, Ruban AV, Walters RG (1996) Regulation of light harvesting in green plants. Annu Rev Plant Physiol Plant Mol Biol **47:** 655–684

Iserles A (1996) A First Course in the Numerical Analysis of Differential Equations. Cambridge University Press, Cambridge, UK

Joliot P, Lavergne J, Beal D (1992) Plastoquinone compartmentation in chloroplasts. I. Evidence for domains with different rates of photo-reduction. Biochim Biophys Acta **1101:** 1–12

Joliot P, Vermeglio A, Joliot A (1993) Supramolecular membrane protein assemblies in photosynthesis and respiration. Biochim Biophys Acta **1141:** 151–174

Krause GH, Weis E (1991) Chlorophyll fluorescence and photosynthesis: the basics. Annu Rev Plant Physiol Plant Mol Biol **42:** 313–349

Krieger A, Weis E (1992) Energy-dependent quenching of chlorophyll-a fluorescence: the involvement of proton-calcium exchange at photosystem 2. Photosynthetica **27:** 89–98

Krieger A, Weis E (1993) The role of calcium in the pH-dependent control of photosystem II. Photosynth Res **37:** 117–130

Laisk A (1993) Mathematical modelling of free-pool and channelled electron transport in photosynthesis: evidence for a functional supercomplex around photosystem I. Proc R Soc Lond B **251:** 243–251

Laisk A, Eichelmann H (1989) Towards understanding oscillations: a mathematical model of the biochemistry of photosynthesis. Philos Trans R Soc Lond **323:** 369–384

Laisk A, Eichelmann H, Oja V, Eatherall A, Walker DA (1989) A mathematical model of the carbon metabolism in photosynthesis: difficulties in explaining oscillations by fructose 2,6-bisphosphatase. Proc R Soc Lond B **237:** 389–415

Laisk A, Kiirats O, Oja V, Gerst U, Weis E, Heber U (1992) Analysis of oxygen evolution during photosynthetic induction and in multiple-turnover flashes in sunflower leaves. Planta **186:** 434–441

Laisk A, Walker DA (1989) A mathematical model of electron transport. Thermodynamic necessity for photosystem II regulation: "light stomata." Proc R Soc Lond B **237:** 417–444

Lavergne J, Trissl HW (1995) Theory of fluorescence induction in photosystem II: derivation of analytical expressions in a model including exciton-radical-pair equilibrium and restricted energy transfer between photosynthetic units. Biophys J **68:** 2474–2492

Osmond CB (1994) What is photoinhibition? Some insights from comparisons of shade and sun plants. *In* NR Baker, JR Bowyer, eds, Photoinhibition of Photosynthesis from Molecular Mechanisms to the Field. BIOS Scientific Publishers, Oxford, UK, pp 1–24

Owens TG (1994) Excitation energy transfer between chlorophylls and carotenoids: a proposed molecular mechanism for non-photochemical quenching. *In* NR Baker, JR Bowyer, eds, Photoinhibition of Photosynthesis from Molecular Mechanisms to the Field. BIOS Scientific Publishers, Oxford, UK, pp 95–110

Prasil O, Adir N, Ohad I (1992) Dynamics of photosystem II: mechanism of photoinhibition and recovery processes. *In* J Barber, ed, Topics in Photosynthesis, Vol 11. The Photosystems: Structure, Function and Molecular Biology. Elsevier, Amsterdam, pp 295–348

Price GD, Yu JW, von Caemmerer S, Evans JR, Chow WS, Anderson JM, Hurry V, Badger MR (1995) Chloroplast cytochrome b6/f and ATP synthase complexes in tobacco: transformation with antisense RNA against nuclear-encoded transcripts for the Rieske FeS and ATP(delta) polypeptides. Aust J Plant Physiol **22:** 285–297

Renger G (1992) Energy transfer and trapping in photosystem II. *In* J Barber, ed, Topics in Photosynthesis, Vol 11. The Photosystems: Structure, Function and Molecular Biology. Elsevier, Amsterdam, pp 45–100

Schreiber U, Neubauer C (1987) The polyphasic rise of chlorophyll fluorescence upon onset of strong continuous illumination. II. Partial control by the photosystem II donor side and possible ways of interpretation. Z Naturforsch **42c:** 132–141

Schreiber U, Neubauer C (1990) O_2-dependent electron flow, membrane energization and the mechanism of non-photochemical quenching of chlorophyll fluorescence. Photosynth Res **25:** 279–293

Ting CS, Owens TG (1993) Photochemical and nonphotochemical fluorescence quenching processes in the diatom *Phaeodactylum tricornutum.* Plant Physiol **101:** 1323–1330

Ting CS, Owens TG (1994) The effects of excess irradiance on photosynthesis in the marine diatom *Phaeodactylum tricornutum.* Plant Physiol **106:** 763–770

van Grondelle R, Dekker JP, Gillbro T, Sundström V (1994) Energy transfer and trapping in photosynthesis. Biochim Biophys Acta **1184:** 1–65

van Mieghem F, Brettel K, Hillmann B, Kamlowski A, Rutherford AW, Schlodder E (1995) Charge recombination reactions in photosystem II. 1. Yields, recombination pathways, and kinetics of the primary pair. Biochemistry **34:** 4798–4813

Weis E, Berry JA (1987) Quantum efficiency of photosystem II in relation to "energy" dependent quenching of chlorophyll fluorescence. Biochim Biophys Acta **894:** 198–208